Available online at www.sciencedirect.com

SCIENCE DIRECT®

ELSEVIER

Chemical Physics Letters 381 (2003) 129–138

CHEMICAL PHYSICS LETTERS

www.elsevier.com/locate/cplett

Simulating dissipative phenomena with a random phase thermal wavefunctions, high temperature application of the Surrogate Hamiltonian approach

David Gelman, Ronnie Kosloff *

Department of Physical Chemistry, Fritz Haber Research Center for Molecular Dynamics, Hebrew University of Jerusalem, Jerusalem 91904, Israel

Received 20 July 2003; in final form 18 September 2003

Abstract

A scheme for calculating thermally averaged observables for quantum dissipative systems is presented. The method is based on a wavefunction with equal amplitude and random phase composed of a complete set of states, which is then propagated in imaginary time $\beta/2$. Application to a Surrogate Hamiltonian simulation of a molecule subject to an ultrafast pulse coupled to a bath is studied. Compared to Boltzmann thermal averaging the method scales more favorably with an increase in the number of bath modes. A self-averaging phenomenon was identified which reduces the number of random sets required to converge the thermal average.
© 2003 Elsevier B.V. All rights reserved.

1. Introduction

Modeling quantum dissipative phenomena remains a challenging problem in condensed matter physics and chemistry [1]. Among other approaches the Surrogate Hamiltonian method [2] has been developed to describe the short time quantum dynamics of dissipative processes, that take place on metal surfaces. Recently, the method was extended to model an ultrafast charge transfer processes in condensed matter [3,4].

The method is based on constructing a surrogate finite system-bath Hamiltonian, that in the limit of an infinite number of bath modes reproduces the true system dynamics. This is done by renormalizing the system-bath interaction term in the Surrogate Hamiltonian. Since within a finite interval of time, the system cannot resolve the full density of the bath states, it is sufficient to replace the bath modes by a finite set. The Surrogate Hamiltonian, consisting of a finite number of bath modes, faithfully represents the dynamics of the observable system for a finite time. This construction is not Markovian and differs from the Redfield [5,6] or semigroup treatments [7–9]. The use of a finite number of bath modes limits the length of time in which the dynamics is consistent

---

* Corresponding author. Fax: +97226513742.
E-mail addresses: davg@fh.huji.ac.il (D. Gelman), ronnie@fh.huji.ac.il (R. Kosloff).

doi:10.1016/j.cplett.2003.09.119

with that of a "true" infinite bath. This makes the Surrogate Hamiltonian method well suited for short time events.

The application of the Surrogate Hamiltonian method has been practically restricted to the low temperature regime. For finite temperatures a Boltzmann average is needed. However, the Hilbert space of the total system $\mathscr{H}_{\mathrm{S}} \otimes \mathscr{H}_{\mathrm{B}}$ contains many more states than the Hilbert space of the primary system alone, $\mathscr{H}_{\mathrm{S}}$. Therefore computing the large number of eigenstates and then repeating the propagation step for each initial state has limited the use of the Surrogate Hamiltonian. The number of eigenfunctions required grows with temperature, and what is more important, it grows exponentially as the number of bath modes increases.

In this Letter we present an alternative scheme of calculating thermally averaged properties suitable for the Surrogate Hamiltonian method. The method is based on a random phase superposition of all states in the combined Hilbert space $\mathscr{H}_{\mathrm{S}} \otimes \mathscr{H}_{\mathrm{B}}$. By averaging a sum of projections of these superpositions the identity operator can be reconstructed for any basis set. Applying the thermal propagator $\mathrm{e}^{-\beta/2\hat{\mathbf{H}}_0}$ to this state, a thermal wavefunction is produced. This pure state serves as an initial state for the time propagation and for the evaluation of the primary system observables. Averaging of many random phase sets leads to the thermal averaged observables. For scattering problems, a thermal Gaussian wavepackets defined by a width which is adjusted to the mean kinetic energy of a free particle thermal ensemble has been employed [10,11]. A uniform averaging in coordinate space would lead to a thermal free particle density operator [10]. These application are non-random and are limited to free space. The random phase vectors have been used before by [12] in order to calculate the linear response functions of non-interacting electrons with a time-dependent Schrödinger equation.

The scaling of computation effort with the temperature and the number of the bath modes is more favorable for the proposed random method compared to direct thermal averaging over the energy eigenstates. Comparable results are obtained by repeating a relatively small number of propagations. In addition since the random phase wavepacket can be expanded in any set of states, the calculation of the energy eigenstates becomes unnecessary.

The random phase method was tested for the model of Morse oscillator in equilibrium with an ohmic bath, perturbed by a short pulse. The absorbed power and dipole correlation function were calculated for a relatively high temperature with an increasing number of the bath modes. The results obtained from the random phase thermal averaging were compared with the results from a direct averaging using the eigenstates of the combined system-bath.

2. Method

2.1. The thermal wavefunction

The initial state of a quantum encounter at finite temperature is described by the mixed state density operator

$$\hat{\boldsymbol{\rho}}_\beta(0) = \frac{\mathrm{e}^{-\beta\hat{\mathbf{H}}_0}}{Z} \tag{1}$$

with $\beta = 1/k_bT$, $\hat{\mathbf{H}}_0$ the stationary Hamiltonian and $Z = \mathrm{Tr}\{\mathrm{e}^{-\beta\hat{\mathbf{H}}_0}\}$ is the partition function. The density operator is diagonal in the energy representation therefore

$$\hat{\boldsymbol{\rho}}_\beta = Z^{-1}\sum_{j=1}^{L} \mathrm{e}^{-\beta E_j}|\psi_j\rangle\langle\psi_j| \tag{2}$$

with $Z = \sum_j^L \mathrm{e}^{-\beta E_j}$, L is the dimension of the Hilbert space $\mathscr{H}$. E_j is the energy of the jth eigenfunction $|\psi_j\rangle$. An evaluation of Eq. (2) by direct diagonalization of $\hat{\mathbf{H}}_0$ would scale as $\mathrm{O}(L^3)$. For a finite temperature, employing propagation techniques [13] Eq. (2) can be approximated using only J energy eigenfunctions $|\psi_j\rangle$ with Boltzmann weights where J is chosen such that $\mathrm{e}^{-\beta E_J} \ll \epsilon$, where ϵ is the error. In this case the numerical effort is close to $\mathrm{O}(J^3)$. In the application of interest, the Surrogate Hamiltonian, cf. Section 2.2, both L and J scale exponentially with the simulation time. These scaling relations are the motivation for seeking an alternative method for thermal averaging.

The starting point is a wavefunction composed of a complete set of eigenfunctions $\{|\phi\rangle\}$ with equal amplitude and a random set of phases $\vec{\theta}$:

$$|\Phi(\vec{\theta})\rangle = \sqrt{Q}\sum_{k=1}^{L} \mathrm{e}^{\mathrm{i}\theta_k}|\phi_k\rangle, \tag{3}$$

where $\sqrt{Q}$ is a normalization constant. The projection constructed from this wavefunction

$$|\Phi(\vec{\theta})\rangle\langle\Phi(\vec{\theta})| = Q\sum_{n,m} \mathrm{e}^{\mathrm{i}(\theta_n-\theta_m)}|\phi_n\rangle\langle\phi_m| \tag{4}$$

connects all states in the Hilbert space. Using the property of the average of random phases

$$\left\langle \mathrm{e}^{\mathrm{i}(\theta_n-\theta_m)}\right\rangle = \frac{1}{2\pi}\int_0^{2\pi} \mathrm{e}^{\mathrm{i}(n-m)\theta}\,\mathrm{d}\theta = \delta_{nm}, \tag{5}$$

the off-diagonal elements of the projection Eq. (4) can be eliminated. This property is used to obtain the identity operator $\hat{\mathbf{I}}$ by averaging many realizations of the projection with different phase sets $\vec{\theta}$:

$$\hat{\mathbf{I}} = \lim_{K\to\infty}\left(\frac{1}{K}\sum_{k=1}^{K}|\Phi(\vec{\theta}_k)\rangle\langle\Phi(\vec{\theta}_k)|\right), \tag{6}$$

where $\vec{\theta}_k$ is the kth realization of the random phase set $\vec{\theta}$. This identity can be employed to construct the thermal state by averaging an ensemble of random thermal wavefunctions

$$\begin{aligned}\hat{\boldsymbol{\rho}}_\beta &= \frac{1}{Z}\mathrm{e}^{-(\beta/2)\hat{\mathbf{H}}_0}\hat{\mathbf{I}}\mathrm{e}^{-(\beta/2)\hat{\mathbf{H}}_0}\\ &= \lim_{K\to\infty}\frac{1}{Z}\left(\frac{1}{K}\sum_{k=1}^{K}\left|\Phi\left(\frac{\beta}{2},\vec{\theta}_k\right)\right\rangle\left\langle\Phi\left(\frac{\beta}{2},\vec{\theta}_k\right)\right|\right),\end{aligned} \tag{7}$$

where the random thermal wavefunction becomes

$$\left|\Phi\left(\frac{\beta}{2},\vec{\theta}\right)\right\rangle = \mathrm{e}^{-(\beta/2)\hat{\mathbf{H}}_0}|\Phi(\vec{\theta})\rangle. \tag{8}$$

The advantage of Eq. (8) is that the random thermal wavefunction can be obtained by propagating an initial random phase wavefunction in imaginary time $\beta/2$. Using this construction a thermal average of an observable $\langle\hat{\mathbf{A}}\rangle_\beta$ becomes

$$\begin{aligned}\langle\hat{\mathbf{A}}\rangle_\beta &= \mathrm{tr}\{\hat{\boldsymbol{\rho}}_\beta\hat{\mathbf{A}}\}\\ &= \lim_{K\to\infty}\frac{1}{Z}\left(\frac{1}{K}\sum_{k=1}^{K}\left\langle\Phi\left(\frac{\beta}{2},\vec{\theta}_k\right)\right|\hat{\mathbf{A}}\left|\Phi\left(\frac{\beta}{2},\vec{\theta}_k\right)\right\rangle\right).\end{aligned} \tag{9}$$

The random approach to the thermal-averaged observable is subject to statistical errors. If the realizations are statistically independent, the standard error of the mean value decreases with the square root of the number of random phase sets

$$\sigma^2 = \frac{\lambda(L)}{K}, \tag{10}$$

where $\lambda(L)$ takes into account the dependence of the statistical error on the Hilbert space size L and temperature T, but does not depend on the number of random sets K. Using a sufficiently large number of simulations, $\lambda(L)$ can be determined, as well as the number of random phase sets which are necessary to achieve a given accuracy σ. The dependence of $\lambda(L)$ on the system size can be related to the degree of self-averaging of the observable [14]. If $\lambda(L)$ is a non-increasing function of L with an increase in system size, the random method will become more efficient than the direct Boltzmann thermal averaging.

2.2. Brief review of the Surrogate Hamiltonian method

The system under study describes a primary system immersed in a bath. The state of the combined system-bath is described by the wave function $\Psi(R,\sigma_1,\sigma_2,\ldots,\sigma_{2^M})$, where R represents the nuclear configuration of the dynamical system, and σ_m the bath degrees of freedom. The stationary Hamiltonian of such a combined system is

$$\hat{\mathbf{H}}_0 = \hat{\mathbf{H}}_\mathrm{S}\otimes\hat{\mathbf{I}}_\mathrm{B} + \hat{\mathbf{I}}_\mathrm{S}\otimes\hat{\mathbf{H}}_\mathrm{B} + \hat{\mathbf{H}}_\mathrm{SB}. \tag{11}$$

The primary system Hamiltonian takes the form

$$\hat{\mathbf{H}}_\mathrm{S} = \hat{\mathbf{T}} + V_\mathrm{S}(\hat{\mathbf{R}}), \tag{12}$$

where $\hat{\mathbf{T}} = \hat{\mathbf{P}}^2/2M$ is the kinetic energy and V_S is an external potential, which is a function of the system coordinate(s) $\hat{\mathbf{R}}$. $\hat{\mathbf{H}}_\mathrm{B}$ denotes the dissipative bath Hamiltonian consisting of an infinite sum of spin modes

$$\hat{\mathbf{H}}_\mathrm{B} = \sum_m \varepsilon_m\hat{\boldsymbol{\sigma}}_m^\dagger\hat{\boldsymbol{\sigma}}_m, \tag{13}$$

where ε_m are the representative energy eigenvalues, and $\hat{\boldsymbol{\sigma}}_m$ are the creation and annihilation operators of the representative mode m. More than one effective bath can be employed, each related to a different dissipative phenomenon. As an example a system-bath coupling inducing vibrational dissipation has the form

$$\hat{\mathbf{H}}_{\mathrm{SB}} = f(\hat{\mathbf{R}}) \otimes \sum_m d_m(\hat{\boldsymbol{\sigma}}_m^\dagger + \hat{\boldsymbol{\sigma}}_m), \tag{14}$$

where $f(\hat{\mathbf{R}})$ is a function of the system displacement operator. The constants d_m are determined from the spectral density $\bar{J}(\varepsilon_m)$:

$$d_m = \sqrt{\bar{J}(\varepsilon_m)/\rho(\varepsilon_m)}, \tag{15}$$

where $\rho(\varepsilon_m)$ is the density of states of the bath.

The observables are associated with operators of the primary system. They are determined from the reduced system density operator: $\hat{\boldsymbol{\rho}}_{\mathrm{S}}(\hat{\mathbf{R}}, \hat{\mathbf{R}}') = \mathrm{tr}_{\mathrm{B}}\{|\Psi(\hat{\mathbf{R}})\rangle\langle\Psi(\hat{\mathbf{R}}')|\}$, where $\mathrm{tr}_{\mathrm{B}}\{\}$ is a partial trace over the bath degrees of freedom That is, the system density operator is constructed from the total system-bath wave function.

The combined system is initiated in a stationary thermal equilibrium state. The dynamics is induced by an external time-dependent perturbation

$$\hat{\mathbf{H}} = \hat{\mathbf{H}}_0 + \hat{\mathbf{H}}_{\mathrm{int}}(t) \otimes \hat{\mathbf{I}}_{\mathrm{B}}. \tag{16}$$

For an excitation by an electromagnetic field, the interaction is described by the time-dependent Hamiltonian

$$\hat{\mathbf{H}}_{\mathrm{int}}(t) = -\hat{\boldsymbol{\mu}} \cdot \hat{\mathbf{E}}(t), \tag{17}$$

where $\hat{\boldsymbol{\mu}}$ denotes the dipole moment operator and $\hat{\mathbf{E}}(t)$ is an external electric field. Any coupling to the bath degrees of freedom is neglected.

The main idea of the Surrogate Hamiltonian method is that the infinite bath is replaced by a finite number of representative modes. Since within a finite interval of time, the system cannot resolve the full density of the bath states, it is sufficient to replace the bath modes by a finite set. The sampling density in energy of this set is determined by the inverse of the time interval. The existence of the spectral density points the way to a convergent method of sampling the bath by a finite number of modes. The finite bath of M spins is constructed with a system-bath coupling term which in the limit $M \to \infty$ converges to the given spectral density of the full bath. The Surrogate Hamiltonian, consisting of a finite number of bath modes, faithfully represents the dynamics of the observable system for a finite time. Higher order system-bath coupling schemes describing dephasing have also been developed [3].

2.3. Numerical details

The state of the system combined with the bath is described by a 2^M-dimensional spinor $\Psi(\hat{\mathbf{R}})$ with M being the number of the bath modes. In the case of a one mode bath $M = 1$, for example, the total wavefunction is represented as a two-component spinor

$$\Psi(\hat{\mathbf{R}}) = \begin{pmatrix} \phi_0(\hat{\mathbf{R}}) \\ \phi_1(\hat{\mathbf{R}}) \end{pmatrix}.$$

The “0” component corresponds to spin down while the “1” component to spin up. Each spinor component $\phi_m(\hat{\mathbf{R}})$ is defined on the equally spaced grid with N grid points. The spinor is bit-ordered, and for the general M case, the mth bit set in the spinor index corresponds to the mth two-level-system (TLS) mode excited where the counting of bits starts at $m = 0$. The wave function representation is designed to perform sums of spin operators efficiently. The detailed algorithm for applying the bath operators has already been given for the general case of an M mode bath [2,3]. The numerical effort scales quasi-linearly ($L \log L$) in the number of spinor components. The algorithm contains all possible system-bath correlations it is also possible to restrict the number of simultaneous bath excitations [4].

The primary system is represented by the Fourier method [15], which allows a faithful description of multidimensional systems with arbitrary potential shapes. The dynamics of the system combined with the bath is generated by solving the time-dependent Schrödinger equation

$$|\Psi(t)\rangle = \hat{\mathbf{U}}(t)|\Psi(0)\rangle = \mathrm{e}^{-\mathrm{i}\hat{\mathbf{H}}t}|\Psi(0)\rangle. \tag{18}$$

The system observables are determined from the reduced system density operator

$$\hat{\boldsymbol{\rho}}_s(t) = \mathrm{Tr}_{\mathrm{B}}\{\hat{\mathbf{U}}(t)|\Psi(0)\rangle\langle\Psi(0)|\hat{\mathbf{U}}^\dagger(t)\}, \tag{19}$$

where $Tr_B\{\}$ denotes a partial trace over the bath degrees of freedom.

Method A: The numerical implementation of the algorithm is as follows:

1. The first step is to build the initial random phase wavefunction $\Psi(\hat{\mathbf{R}},\vec{\theta})$. On each equally spaced grid point k the wavefunction is assigned a random value $e^{i\theta_k}$, where θ_k is a real number, $0 \leqslant \theta_k \leqslant 2\pi$. Each spinor component is also multiplied by $e^{i\theta_m}$.
2. The random wavefunction $\Psi(\hat{\mathbf{R}},\vec{\theta})$ is propagated for an imaginary time $\beta/2$ by the thermal propagator $e^{-(\beta/2)\hat{\mathbf{H}}_0}$. The Newton propagation technique is used [16]. This random phase wavepacket is normalized, leading to $\Psi(\beta/2,\hat{\mathbf{R}},\vec{\theta})$.
3. The thermal random wavefunction is now used as an initial state for a dynamical simulation propagated in real time. This includes an explicit time dependence of the Hamiltonian induced by an external field. The propagation is cut to short time segments and for each segment $e^{-i\hat{\mathbf{H}}\Delta t}$ is applied. The Chebychev method [13] is used to compute the evolution operator. For time-dependent Hamiltonian, the Chebychev propagator remains stable with a slightly different scaling [17].
4. The relevant dynamical observables of the primary system are calculated.
5. The simulation is repeated, many times, with different sets of initial random wavefunctions (steps 1–4).
6. The final step is to average all the results obtained for different sets of random phases.

Method B: An alternative method for obtaining the random phase wavefunction is based on the assumption that the eigenvalues of $\hat{\mathbf{H}}_0$ are quasi-random. A propagation in real time $e^{-i\hat{\mathbf{H}}_0\tau}$ for a random period τ, will multiply to each eigenvalue component by a random phase $e^{-i\theta_k}$, where $\theta_k = E_k\tau$.

1. A wavefunction is constructed with equal amplitude in all components $\psi(\hat{\mathbf{R}})$.
2. The wavepacket is propagated in imaginary time $\beta/2$ by $e^{-(\beta/2)\hat{\mathbf{H}}_0}$ and normalized, leading to $\psi(\beta/2,\hat{\mathbf{R}})$.
3. The resulting wavefunction is propagated for a random real period $e^{-i\hat{\mathbf{H}}_0\tau}$, leading to $\psi(\tau,\beta/2,\hat{\mathbf{R}})$. The random time is chosen to be on the same order as the simulation periods ($\tau \sim t_{\mathrm{sim}}$).
4. The wavefunction is then used as an initial state for the dynamical simulation where the propagation includes the effect of the external field $e^{-i\hat{\mathbf{H}}\Delta t}$.
5. The process (1–4) is repeated and averaged.

2.4. Numerical scaling

The required computational resources in CPU time of the different thermal averaging methods determines their applicability. The framework for estimating the numerical scaling of the simulation is set by the energy range $\Delta E_{\mathrm{range}} = E_{\max} - E_{\min}$ and the time scale t_{sim}. The elementary step of the simulation is to perform the operation of the Hamiltonian on the wavefunction $\phi = \hat{\mathbf{H}}\psi$. When the Fourier method is used for the primary system, and the Surrogate Hamiltonian method for the bath, the scaling of this elementary step becomes $O(L\log L) = O(2^M M \cdot N\log N)$ [18] (see Table 1).

The zero temperature simulation will serve as a reference to the cost of thermal averaging. There are two steps to the calculation. The first is finding the lowest energy state. This can be done by propagation in imaginary time τ. It is sufficient considering the required energy resolution to propagate to a time scale of $\tau = t_{\mathrm{sim}}$. The number of propagation steps would be $n \approx \frac{1}{2}\sqrt{t_{\mathrm{sim}} \cdot \Delta E_{\mathrm{range}}}$ [13]. The simulation itself would require a larger number of propagation steps of the order of $n \approx \frac{1}{2} t_{\mathrm{sim}} \cdot \Delta E_{\mathrm{range}}$ [19]. The simulation effort will therefore scale as: $O(2^M MN\log N t_{\mathrm{sim}} \cdot \Delta E_{\mathrm{range}})$ or as $O(M2^M) \sim O(2^M)$ with the number of bath modes.

For finite temperature the numerical effort of the direct approach requires obtaining J eigenfunctions and in addition J real time propagations for a period t_{sim} of each eigenvalue. J is determined

Table 1
The notations used herein

Number of grid points	N
Number of bath modes	M
Dimension of $\mathscr{H}_S \otimes \mathscr{H}_B$	$L = N \cdot 2^M$
Number of eigenstates in the direct averaging	J
Number of random phase sets	K

by the condition that the Boltzmann weight is smaller than a tolerance $e^{-\beta E_J}/Z \ll \epsilon$. Assuming an even distribution of eigenvalues $E_J \approx \Delta E_{\text{range}} J/L$, leads to the estimation of J:

$$J \approx 1 + \frac{-k_b \log(\epsilon Z)}{\Delta E_{\text{range}}} LT. \tag{20}$$

In Eq. (20) J scales linearly with temperature T and exponentially $O(2^M)$ with the number of bath modes. If J is small, i.e. $J \leqslant 200$, the total numerical cost is J times the cost of the zero temperature calculation. This means that the numerical cost should scale as $O(2^{2M})$. When J becomes large the cost of obtaining the J eigenfunctions overcomes the cost of propagation. The numerical scaling of eigenfunction selection becomes proportional to $\sim J^3$, leading to an exponential scaling of $O(2^{4M})$ with respect to the number of bath modes. This is the reason that the direct method is practically restricted to low temperature simulations.

The numerical effort of the random phase thermal wavefunction method is split into the computation cost of obtaining the thermal wavefunction and cost of the K propagations of the wavefunction to obtain the thermal averaging. Both random method require an initial propagation in imaginary time $\tau = \beta/2$. The numerical effort is small compared to the real time propagation for $t = t_{\text{sim}}$. The numerical effort in randomization by real time propagation is approximately equivalent to the propagation effort required in the simulation. $\tau = 10\% t_{\text{sim}}$ was found to be sufficient. This means that the numerical effort is K times the effort at zero temperature. The number K can be estimated from Eq. (10) and depends on the functional dependence of $\lambda(L)$ on L. In the analyzed result (cf. Section 3) it was found that due to self averaging $\lambda(L)$ is a decreasing function of L. This means that the numerical scaling of the method with respect to the number of bath modes becomes equivalent to the zero temperature case of $O(2^M)$.

3. Results

The illustrative example chosen to test the methods models a typical simulation of ultrafast spectroscopy in condensed phases. A molecule which is first equilibrated with its solvent is subject to a short EM pulse. In the model the molecule is described as a Morse oscillator $V(\hat{\mathbf{X}}) = D(e^{-2\alpha\hat{\mathbf{X}}} - 2e^{-\alpha\hat{\mathbf{X}}})$ where $\hat{\mathbf{X}} = \hat{\mathbf{R}} - \hat{\mathbf{R}}_{\text{eq}}$, is linearly coupled to the dissipative bath. The bath, assumed to be ohmic, is described by its spectral density

$$\bar{J}(\epsilon) = \gamma \epsilon e^{-\epsilon/\epsilon_c}. \tag{21}$$

The dimensionless parameter γ determines the strength of coupling and ϵ_c is a cutoff frequency. A finite bath with equally spaced sampling of the energy range was used. The primary system parameters were chosen as $D = 0.05$, $\alpha = 2.0$, and $\mu = 10^5$ (all in atomic units).

To simulate directly the absorption spectrum a short electromagnetic pulse is applied to the system. The corresponding electric field has the following time-dependent form:

$$E(t) = \mathscr{E}_0 \sin^2\left[\frac{\pi(t - t_0)}{t_{\text{p}}}\right] \cos(\omega_L t), \tag{22}$$

where $\mathscr{E}_0$ is the electric field amplitude, ω_L is the laser carrier frequency, and t_{p} is the pulse duration. The laser field has the $\sin^2$ form. Other pulse shapes, such a Gaussian resulted in essentially similar results.

The laser parameters were chosen as $\mathscr{E}_0 = 0.001$ a.u. and $t_{\text{p}} = 1000$ fs. The temperature was chosen to be relatively high $k_b T = \omega_0$ ($\omega_0 = \alpha\sqrt{2D/\mu}$), so that at least several of the vibrational energy levels are populated.

3.1. Power absorption

The thermal averaged absorption spectrum was calculated using the methods described above. A non-perturbative direct method is employed applicable to strong or weak fields. The power absorbed or emitted from the radiation field is given by the expectation value [20]

$$\mathscr{P} = \left\langle \frac{\partial \hat{\mathbf{H}}_{\text{int}}}{\partial t} \right\rangle = \text{Tr}_{\text{S}}\left\{ \hat{\boldsymbol{\rho}}_{\text{S}} \frac{\partial \hat{\mathbf{H}}_{\text{int}}}{\partial t} \right\} \tag{23}$$

To obtain the total energy ΔE absorbed by a pulse, Eq. (23) is integrated for the total pulse duration. By varying the carrier frequency ω_L of the pulse and calculating ΔE, a spectrum of absorbed energy vs frequency was obtained.

The bath parameters were chosen as $\gamma = 4.0$ and $\epsilon_c = 1.5\omega_0$ and with a 5-modes bath ($M = 5$), the Surrogate Hamiltonian method converges to a timescale of the pulse duration.

As a reference, the power was calculated directly by finding the first J eigenfunctions of H_0. The simulation including the pulse was run for each eigenfunction and Boltzmann averaged.

For $M = 3$ and $k_bT = \omega_0$ the required number of eigenstates $J \approx 30$, however, for $M = 9$ bath $J \approx 1420$.

The direct thermal averaging results were then compared with the random phase thermal wave-function results. The convergence of the absorbed power with K random phase sets is shown in Fig. 1. For $K > 50$ the agreement between two calculations is quantitatively good. The random nature is demonstrated in Fig. 2 showing that the statistical error decreases linearly with $1/\sqrt{K}$. The function $\lambda(L)$ Eq. (10) which measures the self-averaging property is shown in Fig. 2. The best power dependence fit through the data $\lambda(L) \sim L^{\gamma}$ is found to be $\gamma \approx \frac{1}{2}$, ($0.45 \pm 0.09$ for $k_bT = \omega_0$). which means that the observable $\mathscr{P}$ is self-averaging.

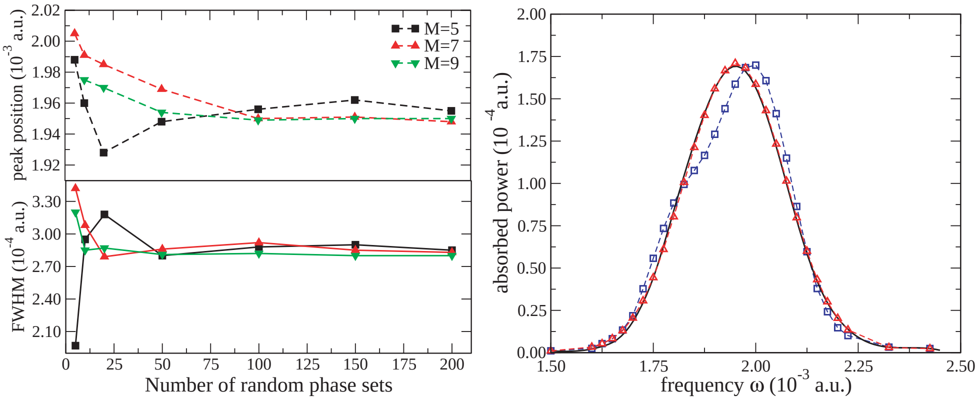

Fig. 1. Convergence of the total absorbed power of the pulse with number of random phase sets. The peak position (top) and FWHN (bottom) of the pulse are shown. The calculations are made for different numbers of bath modes. The thermal averaged absorption is shown for $M = 7$ (right). The solid line refers to the thermal average using the energy eigenstates. The dashed lines with squares and triangles refer to average over 10 and 100 random phase sets, respectively.

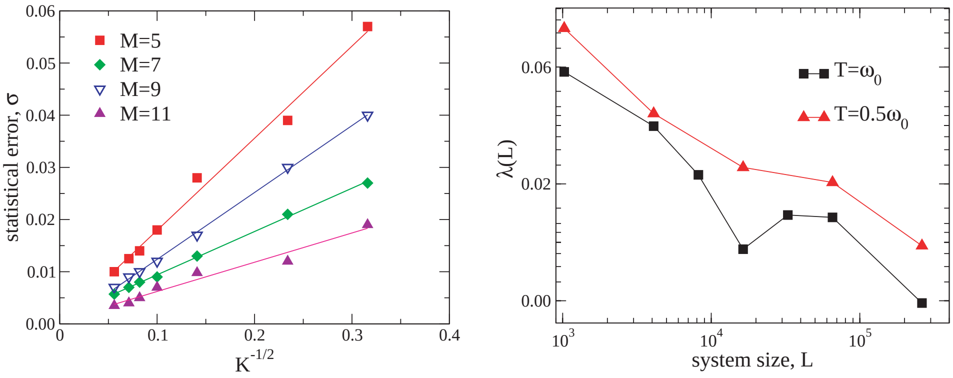

Fig. 2. (Left) The error $\sigma(\mathscr{P})/\langle\mathscr{P}\rangle$ in the power absorbed at $\omega_{\max}$ as a function of $K^{-1/2}$, where K is the number of random phase sets. The calculations are made for an increasing number of bath modes. (Right) The function $\lambda(L)$ versus the system size for two different temperatures.

3.2. Correlation functions

The dipole correlation function is a more stringent test since it depends directly on the dephasing rate. The dipole autocorrelation function was calculated using the Surrogate Hamiltonian without explicitly including the external field

$$C(t) = \mathrm{Tr}_S\{\hat{\boldsymbol{\rho}}_S\hat{\mathbf{M}}\}, \tag{24}$$

where $\hat{\mathbf{M}} = \hat{\boldsymbol{\mu}}^* e^{-i\hat{\mathbf{H}}t}\hat{\boldsymbol{\mu}}e^{i\hat{\mathbf{H}}t}$ and $\hat{\boldsymbol{\mu}} \propto \hat{\mathbf{X}}$ is the actual dipole function.

Fig. 3 shows the dipole autocorrelation function calculated by Eq. (24) for finite temperature. The initial state for the time propagation was chosen as a random phase thermal wavepacket. Then, the initial state was operated on by the position operator of the oscillator and then was propagated in time. The calculations were performed with an increasing number of the bath modes which progressively pushed the converged part of the approximation to longer times. The thermal averaging was performed using an increasing number of the random phase sets. Reasonably accurate results were obtained with $K = 100$ random phase sets.

Fig. 4 shows the the expectation value of the position $\hat{\mathbf{X}}$ of the oscillator after applying the short pulse. The pulse duration was chosen as $t_p = 500$ fs. The bath parameters are the same as with the previous calculations. The convergence was obtained for a relatively large number of sets.

A comparison of the scaling of the numerical effort between the direct and random methods is shown in Fig. 5. The total power absorbed by the system at $\omega_{\max}$ was calculated for two different temperatures and an increasing number of bath modes. The direct thermal averaging shows the expected increase in the numerical effort with the number of bath modes, as well as the increase of numerical effort with temperature. In particular, the number of J grows linearly with increasing the system size L and the temperature T. However, for a larger number of the bath modes $M > 11$, the cost of obtaining the J eigenfunctions should overcomes the cost of propagation. Thus, the total CPU time in the direct method will grow as $O(L^3)$.

The numerical effort required by the random phase method depends on the desired accuracy. The number of the propagations K that are necessary to achieve a given accuracy σ depends on the system size L and the temperature T. Determining $\lambda(L)$ by fitting Eq. (10) to the simulated data, cf. Fig. 2, we found that $K(L)$ decreases with L as $K(L) \sim L^{-1/2}$. This means that, in order to achieve a constant statistical error in the simulation results when the system size L is increased, the

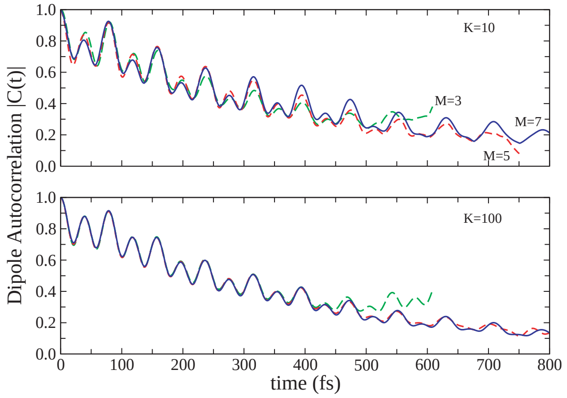

Fig. 3. The absolute value of the dipole autocorrelation function for the relaxing Morse oscillator coupled to the ohmic bath. The dynamics is shown for an increasing number of bath modes ($M = 3, 5, 7$). Upper and lower panels correspond to averaging over a different number of random phase sets ($K = 10$ and $K = 100$, respectively).

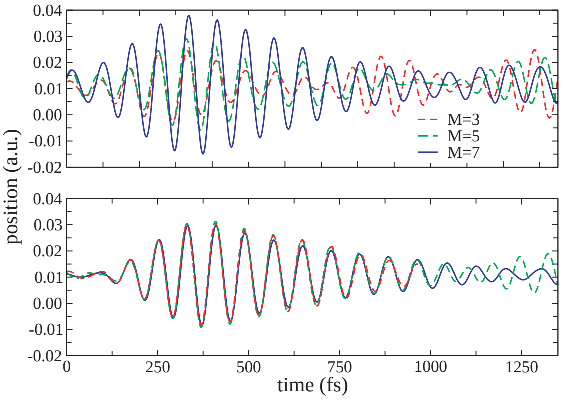

Fig. 4. The expectation value of the position operator vs time. The dynamics is shown for an increasing number of bath modes ($M = 3, 5, 7$). Upper and lower panels correspond to averaging over a different number of random phase sets (10 and 100, respectively).

number of random phase sets K is decreased. It follows that for large system size i.e. a large number of the bath modes M and for high temperature the random phase simulation will always require less CPU time than the direct method. According to Fig. 5 for $k_bT = \omega_0$, the random method becomes more efficient for $M > 6$, and when $k_bT = 0.5\omega_0$ for $M > 7$. The two alternative ways for constructing the random wavepacket gave similar results. The additional computational effort required in method **B** to randomize the phase by real time propagation was found to be insignificant.

A dominant source of computational error in the random phase method is associated with the choice of the initial wavefunction. This wavefunction should consist of equal amplitude of all the states of the combined Hilbert space $\mathscr{H}_S \otimes \mathscr{H}_B$. Good results were obtained by choosing an initial wavefunction as a δ function in coordinates that is located at the minimum of the potential while each spinor component has an equal amplitude and a different phase. The numerical tests also confirm that the actual CPU times follow the scaling arguments.

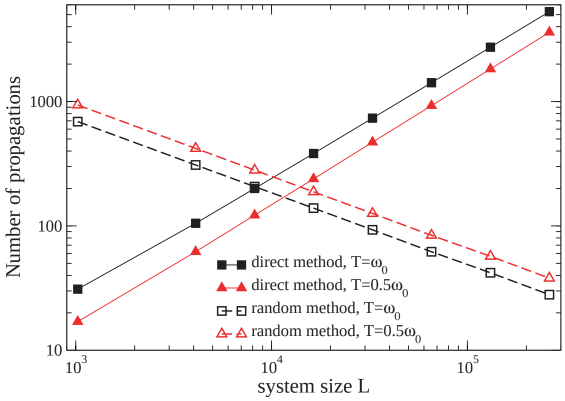

Fig. 5. The numerical effort measured as the number of propagations J or K required for thermal averaging vs the system size L. The figure relates to the power absorbed at $\omega_{\max}$. The temperatures used were $k_bT = \omega_0$ (squares) and $k_bT = 0.5\omega_0$ (triangles). The solid lines refer to the direct method. The dashed lines refer to the number of random phase sets K needed to obtain the converged results with an accuracy of 1%.

4. Discussion

An interesting issue is the source of the observed self averaging. The numerical tests indicate that the size of the statistical pool is $\sim K \cdot L$, this means that there is strong self averaging proportional to the number of states in the Hilbert space. A possible reason is the local character of the observables which depend only on the primary systems operators. For sufficiently strong system-bath coupling we found that the eigenvalue spacing distribution is Wigner like [21]. For weak system-bath coupling a Poisson spacing distribution was found and the self-averaging phenomena was less pronounced. These issues will be the subject of future studies.

The Surrogate Hamiltonian method has been shown to be an effective scheme for simulating quantum transient phenomena taking place in a condensed phase environment. The method is applicable for short time phenomena where the timescale limits the energy resolution of the problem. The original construction was limited to phenomena close to zero temperature. Finite temperature calculations required averaging a substantial number of initial states where the number of these states increased exponentially with the number of bath modes.

The random phase method, introduced in this study, obtains converged results for thermally averaged observables by only averaging a small number of randomly chosen initial states. Moreover the number of initial states K required to obtain convergence is a decreasing function of the system size L for the strong system-bath coupling and decreases with temperature. This finding means that the Surrogate Hamiltonian method has the same scaling properties for the zero temperature simulation as well as for the finite temperature simulations. Moreover the finite temperature simulations can be run in parallel since each random phase run is independent of the others. As a consequence, the Surrogate Hamiltonian method can be applied practically for moderate temperature simulations, when the bath modes do not saturate [22].

It should be mentioned that the present thermal random phase method is not restricted to the Surrogate Hamiltonian approach. The basic construction is representation independent. The random phase method could be applied almost as is to numerical simulations of spin-bath decoherence [23]. The method could also be used for thermal averaging in the multi-configuration time-dependent Hartree application to dissipative dynamics [24].

Acknowledgements

We want to thank Roi Baer for extremely useful discussions. This research was supported by the German-Israel Foundation (GIF). The Fritz Haber Center is supported by the Minerva Gesellschaft für die Forschung, GmbH München, Germany.

References

[1] U. Weiss, Quantum Dissipative Systems, World Scientific, Singapore, 1999.
[2] R. Baer, R. Kosloff, J. Chem. Phys. 106 (1997) 8862.
[3] C.P. Koch, T. Klüner, R. Kosloff, J. Chem. Phys. 116 (2002) 7983.
[4] C.P. Koch, T. Klüner, H.-J. Freund, R. Kosloff, Phys. Rev. Lett. 90 (2003) 117601.
[5] A.G. Redfield, Phys. Rev. 98 (1955) 1787.
[6] A.G. Redfield, IBM J. 1 (1957) 19.
[7] G. Lindblad, Commun. Math. Phys. 48 (1976) 119.
[8] V. Gorini, A. Kossokowski, E.C.G. Sudarshan, J. Math. Phys. 17 (1976) 821.
[9] R. Alicki, K. Lendi, Quantum Dynamical Semigroups and Applications, Springer, Berlin, 1987.
[10] J. Vala, O. Dilieu, F. Masnou-Seeuws, P. Pillet, R. Kosloff, Phys. Rev. A 63 (2000) 013412.
[11] J. Ka, S. Shin, J. Mol. Struct. 623 (2003) 23.
[12] T. Iitaka, S. Nomura, H. Hirayama, X. Zhao, Y. Aoyagi, T. Sugano, Phys. Rev. E 56 (1) (1997) 1222.
[13] R. Kosloff, H. Tal-Ezer, Chem. Phys. Lett. 127 (1986) 223.
[14] A.M. Ferrenberg, D.P. Landau, K. Binder, J. Statist. Phys. 63 (1991) 867.
[15] R. Kosloff, Numerical Grid Methods and Their Application to Schrödinger equation, Kluwer Academic Publishers, The Netherlands, 1993.
[16] G. Ashkenazi, R. Kosloff, S. Ruhman, H. Tal-Ezer, J. Chem. Phys. 103 (1995) 10005.
[17] Y. Huang, D.J. Kouri, D. Hoffman, J. Chem. Phys. 101 (1994) 10497.
[18] R. Kosloff, J. Chem. Phys. 92 (1988) 2087.
[19] R. Kosloff, H. Tal-Ezer, Chem. Phys. Lett. 127 (1986) 223.
[20] R. Kosloff, A.D. Hammerich, D. Tannor, Phys. Rev. Lett. 69 (1992) 2172.
[21] M. Mehta, Random Matrices, second ed., Academic Press, New York, 1991.
[22] D. Gelman, C.P. Koch, R. Kosloff, In preparation.
[23] V.V. Dobrovitski, H.A. De Raedt, Phys. Rev. E 67 (2003) 056702.
[24] N. Nest, H.-D. Meyer, J. Chem. Phys. 119 (2003) 24.